J. Mol. Biol. (1997) **272**, 790–804

JMB

Contributions to Protein Entropy and Heat Capacity from Bond Vector Motions Measured by NMR Spin Relaxation

Daiwen Yang[1], Yu-Keung Mok[2], Julie D. Forman-Kay[2], Neil A. Farrow[1] and Lewis E. Kay[1]*

[1]*Protein Engineering Network Centers of Excellence and the Departments of Medical Genetics, Biochemistry and Chemistry, University of Toronto, Toronto, Ontario Canada, M5S 1A8*

[2]*Biochemistry Research Division, Hospital for Sick Children, 555 University Avenue, Toronto, Ontario Canada, M5G 1X8*

**Corresponding author*

The backbone dynamics of both folded and unfolded states of staphylococcal nuclease (SNase) and the N-terminal SH3 domain from drk (drkN SH3) are studied at two different temperatures. A simple method for obtaining order parameters, describing the amplitudes of motion of bond vectors, from NMR relaxation measurements of both folded and unfolded proteins is presented and the data obtained for ^{15}N-NH bond vectors in both the SNase and drkN SH3 systems analyzed with this approach. Using a recently developed theory relating the amplitude of bond vector motions to conformational entropy, the entropy change between the folded and unfolded forms of SNase is calculated on a per residue basis. It is noteworthy that the region of the molecule with the smallest entropy change includes those residues showing native-like structure in the unfolded form of the molecule, as established by NOE-based experiments. Order parameters of backbone ^{15}N-NH bond vectors show significantly larger changes with temperature in the unfolded states of both proteins relative to the corresponding folded forms. The differential temperature dependence is interpreted in terms of differences in the heat capacities of folded and unfolded polypeptide chains. The contribution to the heat capacity of the unfolded chain from rapid ^{15}N-NH bond vector motions is calculated and compared with estimates of the heat capacity of the backbone unit, -CHCONH-, obtained from calorimetric data. Methyl dynamics measured at 14 and 30°C establish that the amplitudes of side-chain motions in the folded SH3 domain are more sensitive to changes in temperature than the backbone dynamics, suggesting that over this temperature range side-chain ps to ns time-scale motions contribute more to the heat capacity than backbone motions for this protein.

© 1997 Academic Press Limited

Keywords: NMR spin relaxation; order parameters; conformational entropy; heat capacity

Introduction

NMR spectroscopy is a powerful technique for the study of structural and motional properties of macromolecules in solution (Kay *et al.*, 1989; Wüthrich, 1986). This includes investigation of unfolded and partially folded protein states where the dynamical nature of these molecules precludes study using other detailed structural methods, such as X-ray diffraction. Unfolded and partially folded proteins are difficult to study by NMR, however, due to poor chemical shift dispersion (Shortle, 1996). The development of multi-dimensional, multi-nuclear NMR spectroscopy has thus impacted significantly in this area (Bax, 1994; Logan *et al.*, 1994);

Abbreviations used: C_p, heat capacity; drkN SH3, amino-terminal SH3 domain from the protein drk; GuHCl, guanidinium chloride; IPTG, β-D-thiogalactopyranoside; NOE, nuclear Overhauser effect; S^2, square of the order parameter describing the amplitude of ps-ns bond vector dynamics; rmsd, root-mean-squared deviation; R_G, radius of gyration; S_p, contribution to conformational entropy from ps-ns bond vector dynamics; SNase, staphylococcal nuclease; T_1, spin lattice relaxation time; Δ131Δ, partially unfolded form of staphylococcal nuclease where residues 4 to 12 and 141 to 149 of the wild-type protein have been deleted.

0022–2836/97/400790–15 $25.00/0/mb971285

© 1997 Academic Press Limited

backbone ^{15}N and carbonyl (C′) chemical shifts tend to be reasonably well resolved and structural studies that exploit this increased resolution in relation to other nuclei have begun to appear in the literature (Logan *et al.*, 1994; Zhang *et al.*, 1994, 1997a). In particular, we have recently developed a suite of experiments offering improved resolution for the assignment of NOEs in highly overlapped spectra that make use of the resolution of backbone ^{15}N and $^{13}C'$ shifts that are particularly useful for the study of partially unfolded and unfolded proteins (Zhang *et al.*, 1997a).

In addition to structural characterization, NMR can also provide detailed information about the dynamics of proteins through measurement of spin relaxation properties (Alexandrescu & Shortle, 1994; Farrow *et al.*, 1995a, 1997; van Mierlo *et al.*, 1993). Relaxation experiments to date have largely focused on backbone ^{15}N nuclei, but recent methodological advances permit the measurement of backbone ^{13}C (Palmer *et al.*, 1991) and side-chain ^{13}C (LeMaster & Kushlan, 1996) and ^{2}H (Muhandiram *et al.*, 1995) relaxation properties as well. Resolution permitting, it is thus possible to study motional properties of both folded and unfolded states at a variety of positions in the molecule to obtain information that complements structural studies of such systems.

A number of model systems for the study of structure and dynamics in partially folded and unfolded protein states under non-denaturing conditions have been described, including the N-terminal SH3 domain from the *Drosophila* adapter protein drk, drkN SH3 (Zhang & Forman-Kay, 1995), and Δ131Δ, a 131-residue fragment of staphylococcal nuclease (SNase; Alexandrescu *et al.*, 1994) where residues 4 to 12 and 141 to 149 of the wild-type protein have been deleted. In the case of the drkN SH3 domain, the molecule exists in equilibrium between folded (F_{exch}) and unfolded (U_{exch}) states near neutral pH in aqueous buffer, allowing detailed comparison of both states of the molecule under the same set of conditions (Farrow *et al.*, 1995a). Recently, we have also examined the dynamic properties of the drkN SH3 domain in both a fully stabilized state (F_S) through the addition of 0.4 M sodium sulfate and a denatured state (U_{Gdn}) as a result of the addition of 2 M guanidinium chloride (GuHCl). These results have been compared with the dynamics of the F_{exch} and U_{exch} states (Farrow *et al.*, 1997). A particularly interesting conclusion from this study, explored only qualitatively, is that high-frequency (ns to ps) ^{15}N-NH bond vector motions in the folded F_S state of the SH3 domain are significantly less affected by changes in temperature than such motions in the U_{Gdn} denatured state of the protein.

Here, we have investigated this result in more detail by examining the backbone dynamics of the drkN SH3 domain as a function of temperature for both F_S and U_{Gdn} states as well as the temperature-dependence of the side-chain methyl dynamics in the F_S state. In addition, the backbone dynamics have been measured for both the folded SNase and the partially unfolded Δ131Δ at two different temperatures and compared with the results obtained for the SH3 domain. We investigate means of reliable extraction of dynamics parameters from NMR spin relaxation data of unfolded or partially folded molecules, where the frequently used assumption of isotropic motion is likely to be incorrect. A simple method for obtaining order parameters is presented and applied in the analysis of relaxation data measured for the F_S and U_{Gdn} states of the drkN SH3 domain as well as SNase and Δ131Δ. Changes in order parameters have been recast in terms of contributions to changes in conformational entropy using a recently developed theory that relates NMR-derived order parameters and conformational entropy (Yang & Kay, 1996a). In the case of temperature-dependent studies, the change of entropy with temperature allows an estimate of the contributions to the heat capacity of the polypeptide chain from bond vector motions and these results are described. The present study indicates that rapid side-chain motions make a more significant contribution to the heat capacity of the folded drkN SH3 domain than do backbone dynamics over the temperature range of 14 to 30°C.

Obtaining accurate motional parameters describing highly dynamical molecules

Internuclear bond vector dynamics are most often obtained in NMR by heteronuclear spin relaxation studies involving the measurement of X (X=^{15}N, ^{13}C) nucleus T_1 and T_2 relaxation times and steady-state ^{1}H-X NOE values. For a simple two-spin AX spin system, if the relaxation of spin X is dominated by the dipolar interaction between ^{1}H and X and to a lesser extent, by chemical shift anisotropy, neglecting interference effects between these two mechanisms, the relaxation parameters are given by (Abragam, 1961; Kay *et al.*, 1989):

$$1/T_1 = d^2[J(\omega_H - \omega_X) + 3J(\omega_X) + 6J(\omega_H + \omega_X)] + c^2J(\omega_X) \quad (1)$$

$$1/T_2 = 0.5d^2[4J(0) + J(\omega_H - \omega_X) + 3J(\omega_X) + 6J(\omega_H) + 6J(\omega_H + \omega_X)] + (c^2/6)[4J(0) + 3J(\omega_X)] \quad (2)$$

$$\mathrm{NOE} = 1 + d^2\gamma_H/\gamma_X[6J(\omega_H + \omega_X) - J(\omega_H - \omega_X)]T_1 \quad (3)$$

The constants d^2 and c^2 are defined as:

$$d^2 = 0.1\gamma_H^2\gamma_X^2(h/2\pi)^2\langle r_{XH}^{-3}\rangle^2 \quad (4)$$

$$c^2 = (2/15)\omega_X^2(\sigma_\parallel - \sigma_\perp)^2 \quad (5)$$

where h is Planck's constant, γ_H and γ_X are the gyromagnetic ratios of ^1H and X, ω_H and ω_X are the Larmor frequencies of ^1H and X, respectively, r_{XH} is the ^1H-X internuclear distance, and $\sigma_\parallel$ and $\sigma_\perp$ are the parallel and perpendicular components of the (assumed) axially symmetric X chemical shift tensor. Finally, the spectral density function, $J(\omega)$, is given by the cosine Fourier transform of the auto-correlation function, $C(t)$, describing the bond vector motions according to:

$$J(\omega) = \int_{0,\infty} C(t)\cos(\omega t)\,dt \quad (6)$$

A frequently used approach in the analysis of the relaxation data is the method of Lipari & Szabo (1982a,b). In its simplest form, overall isotropic rotation is assumed with a bond vector auto-correlation function given by:

$$C(t) = C_O(t)C_I(t)$$

$$C_O(t) = \exp(-t/\tau_M)$$

$$C_I(t) = S^2 + (1 - S^2)\exp(-t/\tau_e) \quad (7)$$

where $C_O(t)$ and $C_I(t)$ describe the overall and internal dynamics, respectively, S is a generalized order parameter representing the amplitude of internal bond vector motion, and τ_M and τ_e are correlation times describing overall tumbling and internal dynamics, respectively. Equation (7) is strictly valid in the case of a clear separation of the time-scales for overall and internal motions and for isotropic motion.

Not all molecules tumble isotropically, however, and a number of methods have been described in the literature for obtaining dynamical information on molecules that diffuse anisotropically in solution (Broadhurst *et al.*, 1995; Bruschweiler *et al.*, 1995; Tjandra *et al.*, 1995; Zheng *et al.*, 1995). In principle, for a rigid molecule with axial symmetry three correlation times are required to describe rotational diffusion, while in the general case five correlation times are necessary for a rigid ellipsoid (Woessner, 1962). In the case of a flexible system, such as an unfolded protein, the situation is still more complex, since the ensemble consists of a distribution of molecular shapes and it is quite possible that a bond vector connecting the same two atoms in different molecules will therefore orient in solution in very different ways. In addition, the kinetics of exchange between members of the ensemble must also be included in the analysis. A complete analytical solution to the problem is, therefore, extremely difficult. As an approximation, we consider the case where the overall rotation is described by an autocorrelation function of the form:

$$C_O(t) = \sum_{j=1,m} \{a_j \exp(-t/\tau_j)\} \quad (8)$$

where τ_j is the jth correlation time describing overall motion, $\Sigma_{j=1,m}\ a_j = 1$ and the rate of exchange between different members of the ensemble is assumed to be slow compared to $1/\tau_j$. We expect that a description of the dynamics of a particular bond vector in the ensemble of molecules that define the disordered state would involve correlation functions with large numbers of terms (i.e. $C_O(t)$ will be more complex than in the case of an asymmetric rigid molecule, for which $m = 5$). In the limit where the frequency of the internal motions, $1/\tau_e$, satisfies the relation $1/\tau_e \gg 1/\tau_j$, the correlation function can be written as:

$$C(t) = S^2 \sum_{j=1,m} \{a_j \exp(-t/\tau_j)\} + (1 - S^2)\exp(-t/\tau_e) \quad (9)$$

and the corresponding spectral density function is given by:

$$J(\omega) = S^2 \sum_{j=1,m} \{a_j\tau_j/(1 + \omega^2\tau_j^2)\} + (1 - S^2)\tau_e/(1 + \omega^2\tau_e^2) \quad (10)$$

The large number of coefficients that are necessary to describe the overall motion using the spectral density function described by equation (10), which itself is only approximate, suggests that it may well be difficult to extract accurate values of S^2 from a rather limited number of experimental observables. In order to investigate this in some detail, we consider a second-order approximation to $C(t)$, $C^A(t)$, that is exact at times 0 and ∞ and has the following two-exponential form:

$$C^A(t) = S'^2\exp(-t/\tau'_M) + (1 - S'^2)\exp(-t/\tau'_e) \quad (11)$$

The corresponding spectral density function is

$$J^A(\omega) = S'^2\tau'_M/(1 + \omega^2\tau'^2_M) + (1 - S'^2)\tau'_e/(1 + \omega^2\tau'^2_e) \quad (12)$$

In principle, insight into the relation between the values (S'^2, τ'_M and τ'_e, and the dynamics parameters S^2, $\Sigma\ a_j\tau_j$ and τ_e can be obtained by requiring that the spectral density functions $J(\omega)$ and $J^A(\omega)$ be equivalent at three distinct frequencies, for example $J(0) = J^A(0)$, $J(\omega_X) = J^A(\omega_X)$ and $J(\omega_H) = J^A(\omega_H)$. Thus:

$$S'^2\tau'_M + (1 - S'^2)\tau'_e = S^2 \sum_{j=1,m} \{a_j\tau_j\} + (1 - S^2)\tau_e \quad (13)$$

$$S'^2\tau'_M/(1+\omega_X^2\tau'^2_M)+(1-S'^2)\tau'_e/(1+\omega_X^2\tau'^2_e)$$
$$=S^2\sum_{j=1,m}\{a_j\tau_j/(1+\omega_X^2\tau_j^2)\}+(1-S^2)\tau_e/(1+\omega_X^2\tau_e^2) \quad (14)$$

and:

$$S'^2\tau'_M/(1+\omega_H^2\tau'^2_M)+(1-S'^2)\tau'_e/(1+\omega_H^2\tau'^2_e)$$
$$=S^2\sum_{j=1,m}\{a_j\tau_j/(1+\omega_H^2\tau_j^2)\}+(1-S^2)\tau_e/(1+\omega_H^2\tau_e^2) \quad (15)$$

Rather than attempting to solve these complex equations analytically, numerical simulations have been performed to establish the relationship between the parameters defining $J(\omega)$ and $J^A(\omega)$ for the case where X=^{15}N. In particular, 10^4 sets of (S^2, τ_j, τ_e, a_j) ranging from $0.15 \leqslant S^2 \leqslant 1.0$, $2 \leqslant \tau_j \leqslant 15$ ns, $0 \leqslant \tau_e \leqslant 0.3$ ns and $3 \leqslant m \leqslant 20$ ($\Sigma_{j=1,m}\ a_j = 1$) were constructed from which $J(\omega)$ and subsequently ^{15}N T_1, T_2 and ^{1}H-^{15}N NOE values were calculated for a proton frequency of 600 MHz. The T_1, T_2 and NOE values were fit using equations (1) to (3) assuming a simplified spectral density function of the form given in equation (12) and allowing the fitting parameters to vary on a per-residue basis (Alexandrescu & Shortle, 1994; Schurr *et al.*, 1994), i.e. extracted parameters are local. Figure 1 illustrates the relationship between (S'^2, τ'_M, τ'_e) and (S^2, $\Sigma\ a_j\tau_j$, τ_e) for the case where $\tau'_e \leqslant 0.3$ ns. It is clear that the value of τ'_e can overestimate τ_e by a considerable margin. This is the result of the fact that it is not possible to fit the overall tumbling with a single term (τ'_M in equation (12)) and thus τ'_e is increased to compensate. Of much more importance, however, is the good correlation between S^2 and S'^2, as established in the Figure and in Table 1. Not surprisingly, the correlation improves as the distribution of τ_j values decreases. But even for a distribution of τ_j values ranging from 2 to 15 ns, the maximum fractional error in S'^2 relative to S^2 is 11%. As the minimum value of τ_j decreases to approximately 1 ns, the fractional error in S'^2 can be as large as 25%, although if the corresponding value of a_j in this case is less than 0.3, the error decreases to below 13%. We have also noted that for τ'_e values in excess of 0.3 ns the corresponding values of S'^2 can deviate more significantly from S^2. Thus, in the analysis of experimental data, residues for which $\tau'_e \geqslant 0.3$ ns are excluded. Finally, it should be noted that in the context of folded protein states where overall rotation can be described by an axially symmetric diffusion tensor (with components $D_\parallel$ and $D_\perp$), the correlation between S^2 and S'^2 is better than for the situation illustrated in Figure 1, even for $D_\parallel/D_\perp$ ratios as large as 4 or as small as 0.25. This is illustrated in Figure 2.

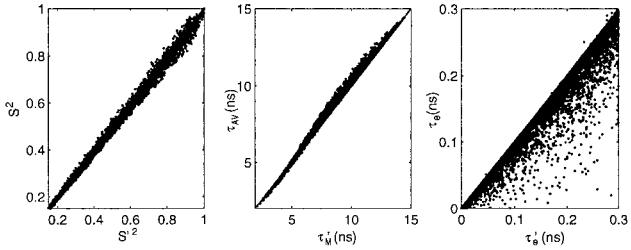

Figure 1. Relation between (S'^2, τ'_M, τ'_e) and (S^2, $\tau_{AV} = \Sigma_{j=1,m}\ a_j\tau_j$, τ_e). The values of (S'^2, τ'_M, τ'_e) are calculated from 10,000 ^{15}N T_1,T_2, NOE data sets (600 MHz ^{1}H frequency) generated assuming a spectral density function described by equation (10) and a distribution of (S^2, τ_j, τ_e) values ranging from $0.15 \leqslant S^2 \leqslant 1.0$, $2 \leqslant \tau_j \leqslant 15$ ns, $0 \leqslant \tau_e \leqslant 0.3$ ns and $m = 4$. Values for which $\tau'_e \geqslant 0.3$ ns are excluded.

These results suggest that for a spectral density function describing the motion of an internuclear vector given by equation (10) and for the distribution of (S^2, τ_j, τ_e) values ranging from $0.15 \leqslant S^2 \leqslant 1.0$, $2 \leqslant \tau_j \leqslant 15$ ns, $0 \leqslant \tau_e \leqslant 0.3$ ns

Table 1. Comparison of S'^2,S^2 and τ'_M,$\tau_{AV} = \Sigma a_j\tau_j$ values for a molecule with overall motion described by equation (9)

m	τ_j distribution range (ns)	Max($\lvert S'^2 - S^2 \rvert / S^2$) (%)	Max($\lvert \tau'_M - \tau_{AV} \rvert / \tau_{AV}$) (%)
4	2–15	11.0	10.0
4	3–15	10.2	9.3
4	6–15	5.8	5.5
4	9–15	2.4	2.3
10	2–15	9.3	8.6
20	2–15	8.9	8.2

In all, 10^4 sets of (S^2, τ_e, a_j) values ranging from $0.15 \leqslant S^2 \leqslant 1.0$, $0 \leqslant \tau_e \leqslant 0.3$ ns, $\Sigma_{j=1,m}\ a_j = 1$ and with the τ_j distribution and values of m given above were constructed from which $J(\omega)$ and subsequently ^{15}N T_1, T_2 and ^{1}H-^{15}N NOE values were calculated (600 MHz ^{1}H frequency) using equations (1) to (3) and (10). Values of S'^2 are obtained by fitting the data using a spectral density of the form given by equation (12). Fitted S'^2 and τ'_e values for which $\tau'_e \geqslant 0.3$ ns were discarded (see the text). The maximum fractional difference between S'^2 and S^2 and between τ'_M and $\Sigma a_j\tau_j$ obtained in each set of 10^4 simulations is reported.

and $3 \leqslant m \leqslant 20$ as described above, it is possible to extract values of S'^2 that have physical meaning (i.e. $S'^2 \sim S^2$ so long as τ'_e does not exceed 0.3 ns). In this approach values of (S'^2,τ'_M,τ'_e) are extracted on a per-residue basis from heteronuclear T_1, T_2 and NOE measurements, as described by Schurr *et al*. (1994) and Alexandrescu & Shortle (1994). Note that these results assume a distribution of correlation times ranging from 2 to 15 ns for the description of overall rotation; a discussion of this assumption is deferred until later. Nevertheless, the approach for data analysis described above is significantly improved over the strategy that we and others have used previously based on fitting the relaxation data of unfolded states with a single global correlation time.

Results and Discussion

Contribution of NH bond vector motion to conformational entropy

The extraction of thermodynamic parameters from NMR spin relaxation data was first described by Palmer and co-workers, who related changes in order parameters associated with the binding of Ca^{2+} to calbindin in terms of changes in free energy (Akke *et al*., 1993). Subsequently we have developed a theory relating conformational entropy changes, ΔS_p, to changes in S^2 (Yang & Kay, 1996a) and a similar study was reported by Wand and co-workers (Li *et al*., 1996). Although the relation between S_p and S^2 was shown to be model-dependent in general, the entropy-order parameter profile calculated from a 1 ns molecular dynamics trajectory of (folded) RNase H1 (Philippopoulos & Lim, 1995) was remarkably well fit assuming a model in which individual bond vectors diffuse in a cone (Yang & Kay, 1996a). This leads to a simple relation describing ΔS_p in terms of the order parameters of bond vector q in states ''*a*'' and ''*b*'', S_a and S_b, respectively, *via*:

$$\Delta S_p(q)/k = \ln\{[3 - (1 + 8S_b)^{1/2}]/[3 - (1 + 8S_a)^{1/2}]\} \quad (16)$$

where k is Boltzmann's constant and $\Delta S_p(q)$ is the change in conformational entropy of bond vector q.

In a previous publication we have calculated the contributions from rapid bond vector motions to the change in conformational entropy arising from the folding/unfolding transition of drkN SH3 (Yang & Kay, 1996a). Figure 3 shows similar results obtained at 32°C for SNase, where ΔS_p is defined as $S_p(\Delta 131\Delta) - S_p$(SNase). There is a significant variability in ΔS_p from residue to residue with an average ΔS_p value of 11.8 J/mol K residue, similar to the value obtained in the case of the drkN SH3 domain (12 J/mol K residue). Of particular interest are the four residues Tyr85, Gly86, Gly88 and Leu89 with significantly below average ΔS_p values. These residues reside in a region corresponding to a turn connecting β-strands 4 and 5 in the folded structure (Loll & Lattman, 1989). Using a suite of recently developed triple resonance experiments for resolving NOEs in poorly dispersed spectra, we observed a number of connectivities in Δ131Δ involving these and neighboring residues that are consistent with native-like structure (Zhang *et al*., 1997b). In particular, (i,$i+6$) NOEs connecting H^α and H^γ of Thr82 with H^α of Gly88, an NN(i,$i+4$) NOE connecting Asp83 and Arg87 and a number of NN(i,$i+3$) NOEs (between Asp83-Gly86 and Tyr85-Gly88) were noted. The (i,$i+6$) NOEs observed in this region are the longest-range NOEs assigned in spectra of Δ131Δ. It is also notworthy that a low ΔS_p value is observed for Gly50. The first 40 residues of Δ131Δ, which comprise three strands of a β-sheet in the native structure, are broadened beyond detection in ^{1}H-^{15}N correlation spectra. This line-broadening has been interpreted in terms of a model in which these residues undergo conformational averaging due to the presence of transient long-range

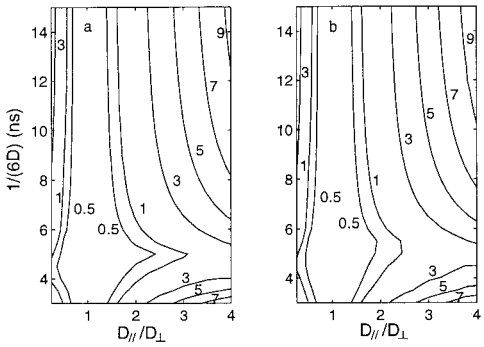

Figure 2. Comparison of τ'_M,τ_{AV} (a) and S'^2, S^2 (b) values for an axially symmetric molecule. The value of τ_{AV} is defined according to $\tau_{AV} = (3\ \cos^2\theta - 1)^2/(24D_\perp) + 3\ \sin^2\theta\cos^2\theta/(5D_\perp + D_\parallel) + 3\ \sin^4\theta/(8D_\perp + 16D_\parallel)$, derived by setting $J(0) = J^A(0)$, where $J^A(0)$ is given by equation (12) and $J(0)$ is given in Tjandra *et al*. (1995) and Woessner (1962). The value of D is given by $D = (D_\parallel + 2D_\perp)/3$. For each value of D and $D_\parallel/D_\perp$ 1000 sets of (θ,S^2,τ_e), where θ describes the orientation of an ^{15}N-^{1}H bond vector relative to the principal axis system of the axially symmetric diffusion tensor with components $D_\parallel$ and $D_\perp$, and $0.15 \leqslant S^2 \leqslant 1.0$, $0 \leqslant \tau_e \leqslant 0.3$ ns were generated from which $J(\omega)$ and subsequently ^{15}N T_1, T_2 and ^{1}H-^{15}N NOE values were calculated (at 600 MHz ^{1}H frequency) using equations given by Woesner (1962). Values of S'^2 and τ'_M are obtained by fitting the data using a spectral density of the form given by equation (12). Fitted S'^2 and τ'_e values for which $\tau'_e \geqslant 0.3$ ns were discarded. To ensure convergence, each fit was performed with two distinct starting points corresponding to initial values of S'^2 of 0.2 and 0.8. If the difference in τ'_M values obtained with these two starting points exceeded 0.01 τ_{AV} the fitted parameters were discarded. The maximum difference between τ'_M and τ_{AV}, $[\mathrm{Max}(|\tau'_M - \tau_{AV}|/\tau_{AV})] \times 100\%$, and between S'^2 and S^2, $[\mathrm{Max}(|S'^2 - S^2|/S^2)] \times 100\%$, obtained in each set of 10^3 simulations is contoured. The step sizes used in contouring are 0.25 for $D_\parallel/D_\perp$ and 0.5 ns for $1/(6D)$.

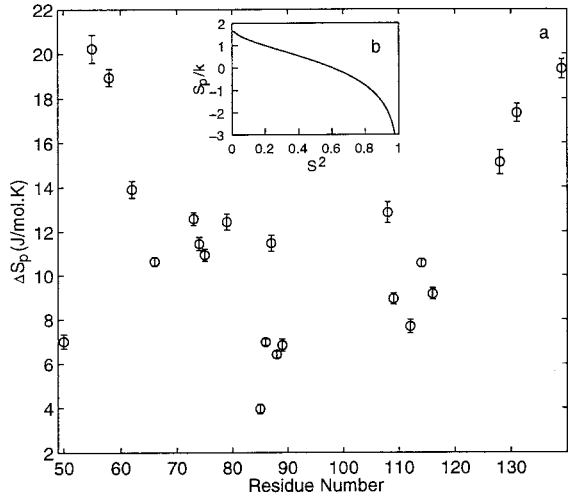

Figure 3. (a) Contributions from rapid ^{15}N-NH backbone bond vector dynamics to the entropy difference, $\Delta S_p = S(\Delta 131\Delta) - S(\text{SNase})$, between Δ131Δ and SNase as a function of residue, calculated from S'^2 values and equation (16). The values of S'^2 were obtained from ^{15}N relaxation data recorded at 32°C. Values of S'^2 in excess of 0.95 were excluded from the calculation (see the text). Vertical error bars are indicated. (b) (inset) Conformational entropy, S_p, as a function of the square of the order parameter, S^2, assuming a model in which bond vectors diffuse freely in a cone. The value of S_p is defined according to $S_p/k = -\int p(q) \ln \{p(q)\}\, dv$, where $p(q)$ is the bond vector probability density and k is Boltzmann's constant (Yang & Kay, 1996a). Note that $S_p(j)$ is the contribution to entropy from bond vector j that depends only on the potential energy function, $U(q)$. It can be shown that although an upper bound for $S_p(j)$ does exist, $S_p(j)$ can indeed be negative (Yang & Kay, 1996a). The total entropy contribution from a particular bond vector (including potential and kinetic energy terms) is non-negative. For a change in entropy that arises exclusively from a change in $U(q)$, the total entropy change is given by ΔS_p.

interactions (Alexandrescu *et al.*, 1994). Residues that are C-terminal to this region also show considerable native-like structure, as established by a number of NH-NH NOEs (connecting Lys48 and Val51, and Lys49 and Glu52). It is thus satisfying to note the correlation between retention of residual native-like structure in Δ131Δ and small ΔS_p values.

It is important to examine how errors in the derived order parameters will affect the accuracy of ΔS_p values, especially given the conditions necessary for S'^2 values to be meaningful (see above). Figure 3b illustrates the relation between S_p/k and S^2, derived assuming bond vector diffusion in a cone (see equation (16)) using classical statistical mechanics. A discussion of the limitations of classical methods relative to quantum mechanical approaches has been given elsewhere (Yang & Kay, 1996a); both methods give identical results for one-dimensional bond vector motion governed by a harmonic potential so long as $S^2 < \sim 0.95$. Figure 3b illustrates that for $0.1 \leqslant S^2 \leqslant 0.7$ the entropy changes relatively slowly with S^2 ($dS_p / dS^2 \sim -2.7\ k$). In contrast the entropy changes more rapidly with order parameter for $S^2 > 0.8$. Thus, although it is more difficult to measure S^2 values accurately in the case of a partially or completely unfolded state, the fact that unfolded proteins are, in general, characterized by order parameters <0.7 where dS_p / dS^2 is reasonably small implies that a larger error in S^2 can be tolerated in measurements of the unfolded state than for the folded molecule, for which S^2 values >0.8 are frequently observed. Fortunately, S^2 values for folded proteins can be measured with great accuracy, typically with errors of only a few percent. Assuming that a given bond vector motion is described by $S^2 = 0.4$ and $S^2 = 0.85$ in the unfolded and folded states, respectively, a 19% error in S^2 (unfolded) results in an 11% error in ΔS_p, while a 3% error in S^2 (folded) leads to the same 11% error in ΔS_p.

Temperature dependence of order parameters

Recently, we have examined the backbone dynamics of the U_{Gdn} and F_S states of the drkN SH3 domain and interpreted the relaxation data in terms of the spectral density values $J(0)$, $J(\omega_N)$ and $J(0.86\ \omega_H)$ (Farrow *et al.*, 1997). We argued that the increase in $J(0.86\ \omega_H)$ that accompanies an increase in temperature (from 14 to 30°C in this study) for the folded state of the protein is largely the result of the concomitant decrease in the overall correlation time of the molecule. In contrast, the increase in $J(0.86\ \omega_H)$ for the U_{Gdn} form of the drkN SH3 domain reflects the increase in internal dynamics that accompanies the higher temperature. Here, we have measured backbone ^{15}N-NH order parameters for the folded SNase and the partially unfolded Δ131Δ mutant at a number of different temperatures and re-examined the data for the U_{Gdn} and F_S states of the drkN SH3 domain in order to obtain S'^2 values as a function of residue. As discussed above, simulations establish that for $0.15 \leqslant S^2 \leqslant 1.0$, $2 \leqslant \tau_j \leqslant 15$ ns and $0 \leqslant \tau_e \leqslant 0.3$ ns, S'^2 values agree well with S^2, so long as $\tau'_e \leqslant 0.3$ ns. Figure 4 illustrates S'^2 *versus* residue for SNase and Δ131Δ at 15 and 32°C, and Figure 5 shows similar results for the F_S and U_{Gdn} states of the drkN SH3 domain at 14 and 30°C. For both Δ131Δ and the U_{Gdn} state of the drkN SH3 domain there is a very noticeable increase in the backbone dynamics at the higher temperature, while the corresponding folded states show much smaller changes. Including only those residues for which order parameters are available at both temperatures, S'^2_{avg} for SNase is 0.86 ± 0.15 and 0.81 ± 0.15 at 15 and 32°C, respectively, with $(\Delta S'^2)_{avg} = 0.045 \pm 0.031$, while S'^2_{avg} is 0.60 ± 0.10 and 0.46 ± 0.09 for the same two temperatures in

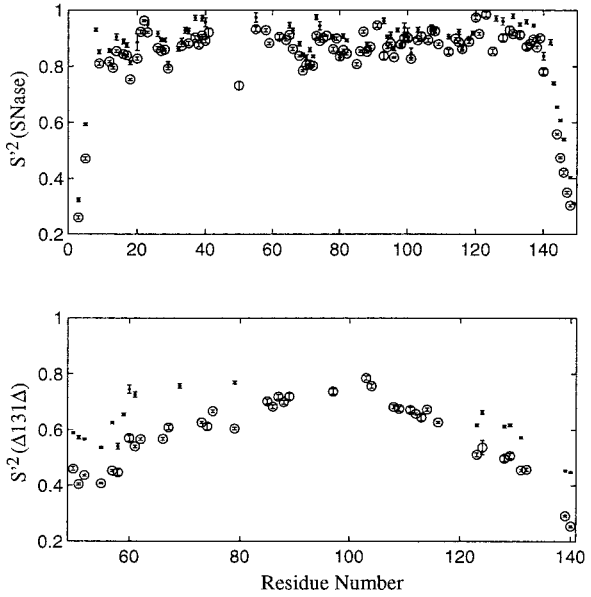

Figure 4. S'^2 values as a function of residue for SNase and Δ131Δ at 15 (●) and 32°C (○). The errors associated with each measurement are indicated with vertical bars.

the case of Δ131Δ ($(\Delta S'^2)_{avg} = 0.143 \pm 0.032$). Similarly, the average values of S'^2 are nearly identical for the F_S state of the drkN SH3 domain at 14°C (0.84 ± 0.05) and 30°C (0.83 ± 0.06) ($(\Delta S'^2)_{avg} = 0.004 \pm 0.036$), while S'^2_{avg} values decrease from 0.48 ± 0.09 (14°C) to 0.40 ± 0.09 (30°C) ($(\Delta S'^2)_{avg} = 0.087 \pm 0.025$) when the domain is denatured in 2M GuHCl. Note that the standard deviation of S'^2 and $\Delta S'^2$ values calculated over all residues have been reported along with the S'^2_{avg} and $(\Delta S'^2)_{avg}$ values above. The average error in S'^2 per residue is 0.01 in all cases. A relatively small number of S'^2 values were obtained for Δ131Δ at 15°C. Interpretation of the relaxation data for many of the residues is complicated by exchange contributions on the ms to μs time-scale. This is established either by the dependence of ^{15}N T_2 values on the spacing between ^{15}N 180° pules in CPMG relaxation experiments or by τ'_e values in excess of 0.3 ns obtained in the fits of the relaxation data. The effects of exchange result in elevated values of both τ'_M and τ'_e; residues for which this is the case are not included in the Figure.

Estimation of the contribution to the heat capacity of the unfolded protein state from NH bond vector motions

One of the most fundamental thermodynamic quantities is the heat capacity of a substance, from which the temperature-dependence of its enthalpy, entropy and free energy can be calculated (Privalov & Gill, 1988) according to:

$$\Delta H_A = \int C_p \, dT$$

$$\Delta S_A = \int C_p \, d\ln T \qquad (17)$$

where ΔH_A and ΔS_A denote the change in enthalpy and entropy of substance A with temperature. Note that for a protein folding reaction the changes in ΔH and ΔS with temperature, ΔH_f and ΔS_f, respectively, are given by:

$$\Delta H_f(Temp^2) = \Delta H_f(Temp^1) + \int_{Temp^1}^{Temp^2} \Delta C_p \, dT \qquad (18)$$

$$\Delta S_f(Temp^2) = \Delta S_f(Temp^1) + \int_{Temp^1}^{Temp^2} \Delta C_p \, d\ln T$$

Although methods based on calorimetry exist for measurement of the heat capacity of both folded and unfolded protein states, as well as the difference in the heat capacities, ΔC_p, of the two states (Gomez *et al.*, 1995; Privalov & Gill, 1988), it is nevertheless important to develop approaches for measuring the relative contributions to heat capacity from the solvent and from conformational entropy of the molecule, from the protein backbone and side-chain moieties and from specific sites in the molecule. In principle, measurement of spin relaxation times as a function of temperature provides a way of addressing some of these issues.

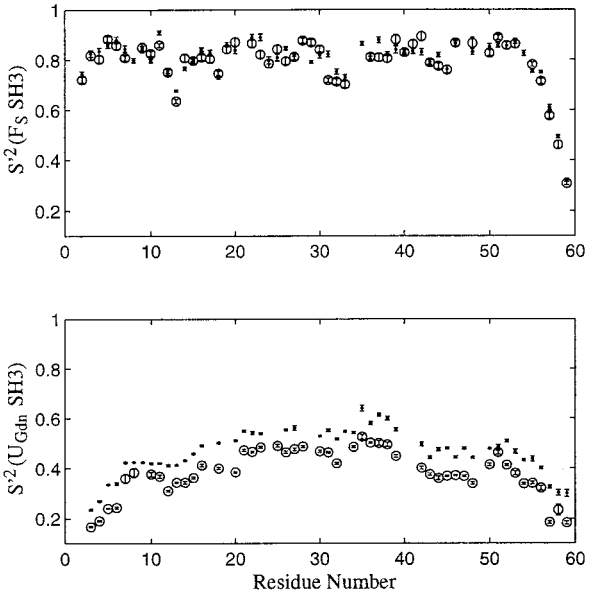

Figure 5. S'^2 values as a function of residue for the F_S and U_{Gdn} states of the drkN SH3 domain at 14 (●) and 30°C (○). The errors associated with each measurement are indicated with vertical bars.

Calorimetric measurements of ΔC_p for a large number of proteins have established that $\Delta C_p > 0$ for the unfolding process and that the magnitude of ΔC_p is related to the hydrophobic surface area that is exposed to solvent upon denaturation (Novokhatny & Ingham, 1994). The majority of the change in heat capacity originates from hydration effects, with a smaller component arising from the differences in conformational entropy between the folded and unfolded states (Makhatadze & Privalov, 1990; Privalov & Makhatadze, 1990). It is also the case, at least over a substantial temperature range, that the contribution to the heat capacity of the unfolded state from protein motions is larger than in the folded form, since the modes available for the unfolded molecule are in general of lower frequency (and larger amplitude) than those in the folded form. This situation is analogous to the variation of the heat capacity of a harmonic oscillator as a function of temperature or vibrational frequency, with C_p increasing both with temperature and with decreasing force constant (Eisenberg & Crothers, 1979). Finally, it is noteworthy that the heat capacity increment for unfolding is itself a function of temperature, with the difference between the heat capacities of folded and unfolded states decreasing with increasing temperature (Privalov & Gill, 1988).

In principle, it is possible to calculate the contribution that the motion of a given bond vector makes to the heat capacity by measuring the temperature-dependence of the dynamics parameters. The results in Figures 4 and 5 suggest that the contributions to the heat capacity from backbone bond vector motions are smaller for the folded protein states considered than for the corresponding unfolded states, since the S'^2 values are significantly more temperature-dependent in the latter case. The heat capacity contribution is readily derived from equation (17) and is given by the relation:

$$C_p = \Delta S/\{\ln(Temp^2/Temp^1)\} \qquad (19)$$

where ΔS is the entropy change calculated from the difference in S^2 values measured for a given bond vector (equation (16)) at the two temperatures, $Temp^2$ and $Temp^1$. Equation (19) assumes that the heat capacity does not vary over the temperature range considered. As mentioned above, calorimetric data have established that this is not the case; however, over a reasonably small temperature range the change in C_p is rather small (Privalov & Makhatadze, 1990). For example, the C_p values for the unfolded and folded forms of lysozyme change from 25.2 to 27.5 kJ/mol K and from 18.2 to 20.0 kJ/mol K, respectively, as the temperature is increased from 5 to 25°C (Privalov & Makhatadze, 1990). Gomez *et al.* (1995) have noted that $\partial C_p/\partial T \sim 4.0 \times 10^{-3}$ J/K^2 g based on calorimetric data obtained for a number of different proteins.

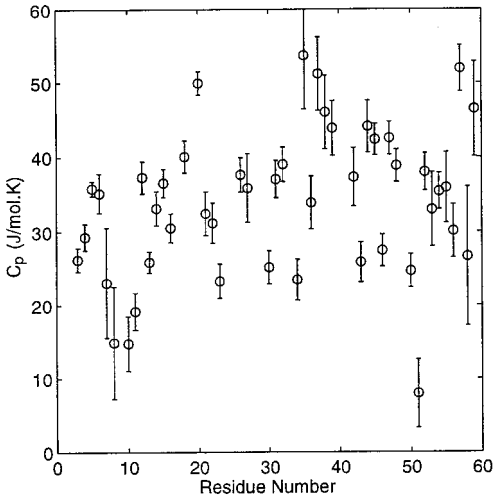

Figure 6. Contributions to the heat capacity (C_p) of the unfolded polypeptide chain (U_{Gdn} state of the drkN SH3 domain) from rapid ^{15}N-NH backbone bond vector motions as a function of residue. The values of C_p were calculated from equation (19) on the basis of S'^2 values measured at 14 and 30°C. There was no S'^2 value $\geqslant 0.95$ at either temperature.

Figure 6 illustrates the contribution to C_p calculated from S^2 values measured at temperatures of 14 and 30°C for the U_{Gdn} state of the drkN SH3 domain. An average value of 34(±10) J/mol K residue (±10 refers to the standard deviation of C_p values measured for all residues and not the error per residue) is obtained and a corresponding value of 59(±17) J/mol K residue is calculated for Δ131Δ measured from data recorded at 15 and 32°C. Average errors in C_p values for the drkN SH3 domain and Δ131Δ are 3 J/mol K residue and 4 J/mol K residue, respectively. In principle, it is also possible to calculate contributions to the heat capacities of folded protein states as well using equation (19). In practice, however, the small differences in S^2 values with temperature for ^{15}N-NH bond vectors in folded proteins coupled with the rapid change of S_p with S^2 for $S^2 > 0.8$ suggests that these C_p estimates will be susceptible to errors; for example C_p values of 2(±39) J/mol K residue and 45(±24) J/mol K residue are calculated for the F_S state of the drkN SH3 domain (temperatures of 14° and 30°C) and SNase (15° and 32°C), respectively, with errors of 20 J/mol K residue and 15 J/mol K residue. In connection with the C_p values estimated for Δ131Δ and the U_{Gdn} state of the drkN SH3 domain, it is interesting to note that Makhatadze & Privalov (1990) estimate the gas phase C_p value of the backbone fragment -CHCONH- to be 56.0 and 58.7 J/mol K at 5 and 25°C, respectively. Although these latter values are obtained on the basis of heat capacity data from small organic molecules and on the assumption that the heat capacity of a substance is given by

the sum of the heat capacities of its constituent parts, it is nonetheless noteworthy that the results obtained by NMR and calorimetric approaches are similar. Note that the NMR method focuses only on contributions from NH bond vectors and thus may well underestimate the C_p value of the -CHCONH- group.

The backbone dynamics presented in Figures 4 and 5 establish that ^{15}N-NH bond vector motions contribute more to the heat capacity of the unfolded protein state than to the corresponding folded state, at least for the two examples considered here. In this context it is interesting to compare the results of this study with those reported for (folded) ribonuclease H in which the temperature-dependence of the backbone dynamics was also studied (Mandel *et al.*, 1996). By measuring the temperature-dependence of $(1-\sqrt{S^2})$ the authors obtain a characteristic temperature for each residue, related to the number of thermally accessible conformational states. High values of the characteristic temperature correspond to small contributions to the heat capacity from dynamics, since an increase in temperature populates few additional states. The authors note that the dynamics of residues in secondary structural elements contribute little to the heat capacity (high characteristic temperature values) and therefore speculate that this may lead to a substantial difference in heat capacity between folded and unfolded states. In contrast, residues in less structured loop and terminal regions have lower characteristic temperatures. These results are consistent with the differences in dynamics between folded and unfolded states that are observed here.

A naive interpretation of the results of Figure 5, in particular, might suggest a larger difference in the heat capacities of unfolded and folded protein states than what is actually observed experimentally by calorimetry. For example, based on data provided by Privalov & Makhatadze (1990) the values of C_p for anhydrous lysozyme at 25°C are 17.2 and 18.5 kJ/mol K for the folded and unfolded states, respectively. In contrast, the average contribution to C_p from ^{15}N-NH bond vector motions in the folded state of the SH3 domain between 14 and 30°C is only 2(±39) J/mol K residue. ($S^2_{avg} = 0.84 \pm 0.05$ (14°C) *versus* $S^2_{avg} = 0.83 \pm 0.06$ (30°C); $\Delta S_{avg} = 0.12 \pm 2.1$ J/mol K residue). It must be noted, however, that the ^{15}N relaxation measurements provide backbone dynamics information only, which clearly must be supplemented by side-chain dynamics studies in order to gain a clear picture of how bond vector motion throughout the molecule contributes to its heat capacity. With this in mind we have also performed methyl dynamics experiments on an ^{15}N, ^{13}C, fractionally ^{2}H-labeled sample of the folded state of the SH3 domain as a function of temperature.

Side-chain methyl order parameters as a function of temperature for the F_S state of the drkN SH3 domain

We have recently developed a method for measuring methyl side-chain dynamics from experiments that record ^{2}H T_1 and $T_{1\rho}$ relaxation times (Muhandiram *et al.*, 1995). Because of the poor resolution and sensitivity of ^{2}H NMR, ^{2}H relaxation properties are measured indirectly through a series of ^{13}C-^{1}H correlation experiments. Signals arising from $^{13}CH_2D$ methyl types are selected with the intensity of individual ^{13}C-^{1}H correlation peaks arising from distinct methyl groups reporting on the relaxation times of the bound deuteron. A detailed account of the theory of the experiment and an application to the C-terminal SH2 domain from phospholipase $C_{\gamma 1}$ both in free and peptide-complexed states have been given previously (Kay *et al.*, 1996; Yang & Kay, 1996b). Figure 7a illustrates the ^{13}C-^{1}H correlation map of a 1.5 mM sample of uniformly ^{15}N, ^{13}C, ~50% ^{2}H-labeled drkN SH3 domain in the F_S state, with only the $^{13}CH_2D$ methyl groups selected. In Figure 7b to d, curves are illustrated corresponding to the decay of $I_ZC_ZD_Z$, $I_ZC_ZD_Y$ and I_ZC_Z magnetization (I=^{1}H, C=^{13}C, D=^{2}H and A_i is the i component of magnetization for spin A) for Ile27$^{\delta 2}$, Ile27$^{\gamma 2}$ and Leu28$^{\delta 2}$.

The values of S^2_{axis} describing the amplitudes of motion of the bond vectors about which the methyl groups rapidly rotate (i.e. the bond connecting the methyl carbon atom and its adjacent carbon atom) are illustrated in Figure 8 for temperatures of 5, 14

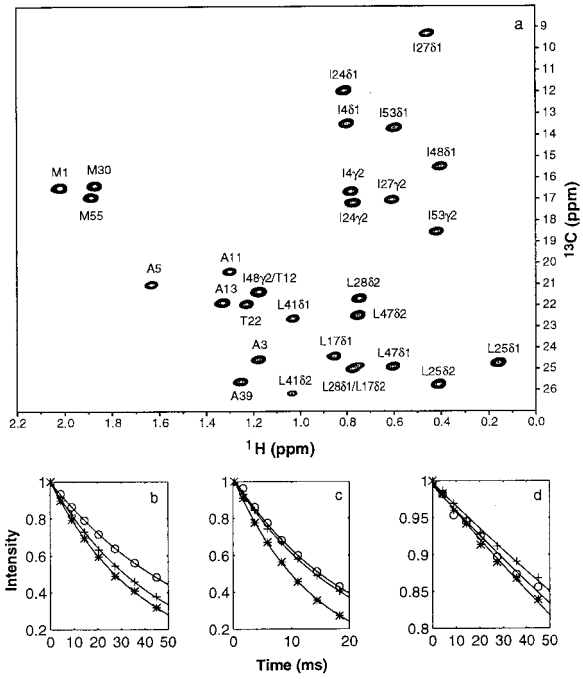

Figure 7. (a) ^{13}C-^{1}H correlation map of the drkN SH3 domain recorded at 30°C, 600 MHz ^{1}H frequency, illustrating correlations involving $^{13}CH_2D$ methyl groups. The decay of $I_ZC_ZD_Z$ (b), $I_ZC_ZD_Y$ (c) and I_ZC_Z (d) for Ile27$^{\delta 2}$ (○), Ile27$^{\gamma 2}$ (*) and Leu28$^{\delta 2}$ (+) are illustrated.

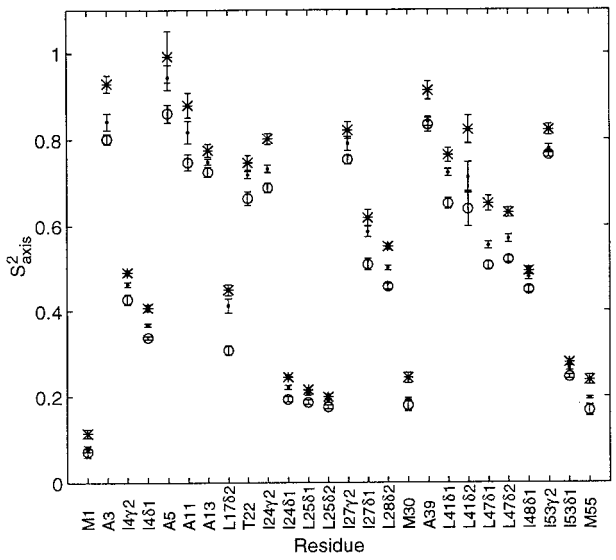

Figure 8. Values of S^2_{axis} obtained from ^{2}H methyl relaxation times, measured at 5 (*), 14 (●) and 30°C (○) for the F_S state of the drkN SH3 domain. Errors in S^2_{axis} are indicated with vertical bars. Values of 9.00 ± 0.06 (5°C), 6.62 ± 0.03 (14°C) and 4.21 ± 0.02 ns (30°C) were used for the overall correlation times.

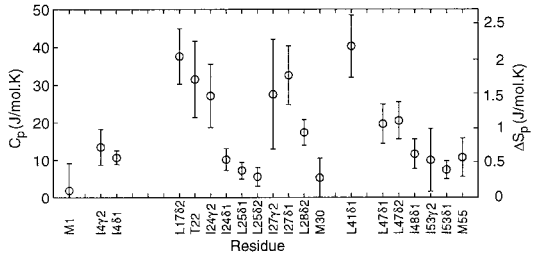

Figure 9. Contributions to the change in conformation entropy and the heat capacity of the F_S state of the drkN SH3 domain arising from differences in the amplitudes of methyl bond vector dynamics at temperatures of 14 and 30°C (see equations (16) and (19)). Ala residues and Leu41$^{\delta 2}$ have been excluded from this analysis, as described in the text.

and 30°C. In all, 26 of 30 residues are represented; cross-peaks from Leu28$^{\delta 1}$ and Leu17$^{\delta 2}$ and from Ile48$^{\gamma 2}$ and Thr12 are overlapped in ^{13}C-^{1}H correlation maps. Note that the values of S^2_{axis} can lie between 0 (complete motional freedom) and 1 (complete restriction). It is clear that, unlike the backbone dynamics measured at 14 and 30°C, the methyl group dynamics of the folded SH3 domain do indeed show a significant temperature-dependence. In addition, the S^2_{axis} values do not always change uniformly with temperature. Figure 9 plots the change in conformational entropy associated with the increased amplitude of motions of the methyl symmetry axis with temperature as reported by the values of S^2_{axis} measured at 14 and 30°C. The corresponding C_p values are also illustrated in Figure 9, with an average value of 17(±12) J/mol K residue (average error of 6 J/mol K residue). An average C_p value of 33(±23) J/mol K residue (average error of 13 J/mol K residue) is obtained from the measurements at 5 and 14°C. Note that ΔS and C_p values are listed for those residues for which S^2_{axis} reports on side-chain bond vector motions (i.e. Ala is omitted). For all but one of the Ala residues, $S^2_{axis} > 0.8$ at one or more temperatures and, as described above, the rate of change of S_p with S^2 increases significantly for S^2 values greater than approximately 0.8, leading potentially to large errors in calculated ΔS and C_p values. In addition, Leu41$^{\delta 2}$ has been removed from analysis because the strong coupling between the C$^{\gamma}$ and C$^{\delta 2}$ carbons atoms leads to an attenuated signal intensity in ^{13}C-^{1}H correlation spectra.

Concluding discussion

NMR spectroscopy is a powerful tool for the characterization of structural and dynamical properties of unfolded and partially folded protein states. However, a significant complication in the analysis of the dynamics of unfolded proteins is that the overall tumbling is not isotropic. The standard analysis of relaxation data based on the simplest form of spectral density function suggested by Lipari & Szabo (1982a,b) is thus not completely appropriate for the interpretation of relaxation times measured on such systems. This has led a number of groups to consider a description of molecular dynamics in terms of the spectral densities themselves (Farrow *et al.*, 1995a,b; Ishima & Nagayama, 1995; Peng & Wagner, 1992). Although a benefit of this approach is that few *a priori* assumptions about the form of the spectral density must be made, regrettably less insight is obtained about the dynamics than from other methods of analysis. With this in mind, we have examined the accuracy of backbone order parameters extracted from ^{15}N relaxation data derived from a motional model in which the overall tumbling is given by a sum of terms with correlation times, τ_j, ranging from 2 to 15 ns. Specifically, we find that assuming a form of $J(\omega)$ given by equation (10) and for (S^2, τ_j, τ_e) ranging from $0.15 \leqslant S^2 \leqslant 1.0$, $2 \leqslant \tau_j \leqslant 15$ ns, $0 \leqslant \tau_e \leqslant 0.3$ ns, S'^2 values can be extracted from fits of the individual residues using a simple Lipari-Szabo (1982a,b) model (equation (12)) that differ by less than approximately 10% from the true S^2 values. Effects of slow time-scale dynamics manifest in large fitted values of τ'_e (equation (12)) and residues for which τ'_e values greater than 0.3 ns are obtained are excluded from further analysis.

Given the fact that the relation between S'^2 and S^2 depends on the distribution of τ_j values it is important to ask whether the distribution considered in the simulations (2 to 15 ns) is reasonable for partially or fully unfolded proteins that can be studied using current NMR techniques. Some assurance comes from small-angle X-ray scattering results that have established that unfolded proteins

are reasonably compact, suggesting that the distribution of correlation times describing tumbling may not be so different from the case of a folded molecule. For example, the radius of gyration (R_G) for ribonuclease A changes from 15 Å in the native state to 19 Å at 51°C upon denaturation by reduction of the four disulfide bonds in the molecule (Sosnick & Trewhella, 1992). Even in 6 M GuHCl, where the R_G of the reduced form of ribonuclease increases to 24 Å, the molecule is still significantly more compact than predicted for a random coil ($R_G > 43$ Å). In the case of a disordered staphylococcal nuclease fragment that differs from the wild-type molecule by the removal of the five C-terminal residues the radius of gyration increases by only a factor of 1.25 relative to that of the native state (Flanagan *et al.*, 1992). Recently, Gillespie & Shortle (1997) have characterized long-range structure in Δ131Δ using a nitroxide spin labeling approach in which 14 samples were prepared, each of which contains a spin label placed in a different site predicted to be on the surface of the denatured molecule. Distances between the spin label and backbone NH protons were estimated on the basis of the decrease in the intensity of cross-peaks in ^{15}N-^{1}H correlation spectra recorded both before and after quenching of the paramagnetic spin label. As the authors point out clearly, the r^{-6} weighting of distances ensures that the restraints obtained will describe a more compact structure than the true average for the ensemble. Nevertheless, the set of structures generated are remarkably similar in overall topology to the structure of the wild-type, suggesting that reasonably compact structures may be generated at least some fraction of the time.

Interpretation of NMR-derived backbone motional parameters of folded proteins is predicated on the assumption that the values of S^2 obtained describe the amplitude of local bond vector motions. Wand and co-workers have extended this idea in their analysis of the main-chain dynamics data for the C-terminal residues of human ubiquitin (Schneider *et al.*, 1992). Assuming that the dynamics of the terminal residues are uncorrelated it is possible to separate the contributions that residue $i-1$ makes to residue i by defining the recursive ratio $S^2(i)/S^2(i-1)$ as describing the amplitude of the local dynamics at site i. In the case of unfolded protein states partially correlated or uncorrelated backbone motions will result in measured S^2 values that are sensitive to both local motions and to motions derived from more distant sites and it is not clear how best to separate such effects when the motion is partially correlated. Thus, values of ΔS_p and C_p calculated on the basis of changes in S^2 as a function of temperature for example, may reflect more than simple differences in local dynamics at the different temperatures. Analysis of molecular dynamics trajectories of unfolded protein states may be informative in this regard and we are currently recording such trajectories.

Order parameters describing motions of backbone ^{15}N-NH bond vectors have been measured for SNase and Δ131Δ as well as for both folded and GuHCl-denatured states of the drkN SH3 domain. The change in entropy between SNase and Δ131Δ is significantly below average for residues retaining native-like structure in Δ131Δ. Strikingly, amplitudes of backbone motions in disordered states, the U_{Gdn} state of the SH3 domain and Δ131Δ, display a more significant temperature-dependence than the corresponding folded forms of the molecules. This difference can be interpreted qualitatively as reflecting differences in contributions to the heat capacities of folded and unfolded protein states from protein motions (i.e. motions in a more rigid folded molecule will contribute less than the lower frequency, larger amplitude motions present in an unfolded protein). Finally, a marked temperature dependence of S^2 is observed for side-chain methyl dynamics in the folded SH3 domain, suggesting that side-chain dynamics may contribute more to the heat capacity than backbone motions for this protein, at least in the range from 14 to 30°C.

Materials and Methods

Protein preparation

Samples of ^{15}N-labeled drkN SH3 domain were prepared as described by Zhang & Forman-Kay (1995). The folded (F_S) and unfolded (U_{Gdn}) states were generated using 0.4 M sodium sulfate and 2.0 M guanidinium chloride, respectively, in buffers of 0.05 M sodium phosphate, 90% H_2O/10% ^2H_2O, pH 6.0 (1 mM protein). An ^{15}N, ^{13}C, ~50% ^{2}H sample of the F_S state of the drkN SH3 domain was prepared as follows: a single colony of *Escherichia coli* BL21 (DE3) carrying the drkN SH3 domain plasmid (Zhang & Forman-Kay, 1995) was inoculated into 50 ml of LB with 100 μg/ml ampicillin. The cells were grown at 37°C for four hours until an A_{600} of approximately 1.1 was achieved. Subsequently, 15 ml of the culture was transferred into 400 ml of M9 medium containing $^{15}NH_4Cl$ and [^{13}C]glucose. The cells were grown to an absorbance of 0.4, spun down and resuspended in 0.4 l of M9 medium containing 50% ^2H_2O, $^{15}NH_4Cl$ (1 g/l) and [^{13}C]glucose (3 g/l). The suspension was diluted five times into 1.6 l of the same medium and grown at 37°C until a final absorbance of 0.8. Protein expression was induced by adding IPTG to a final concentration of 0.25 mg/ml and the cells grown for a further three hours before harvesting. Protein purification was done as described (Zhang *et al.*, 1997a) with the exception that an additional purification step using a MonoQ column (Pharmacia) was employed following gel filtration. Pure protein was dialyzed exhaustively in water, concentrated and lyophilized. The lyophilized powder was resuspended in 50 mM phosphate buffer (pH 6.0) with 10% ^2H_2O and 0.4 M sodium sulfate to give a 1.5 mM NMR sample. Samples of SNase and Δ131Δ were prepared as described by Alexandrescu *et al.* (1994). Sample conditions were: 0.1 mM sodium azide, pH 5.3, 3.5 mM sample.

NMR spectroscopy

NMR experiments were recorded at 15 and 32°C (SNase/Δ131Δ) and at 5, 14 and 30°C (drkN SH3 domain) on a four-channel Varian Inova 600 MHz spectrometer equipped with a *z*-pulsed field gradient unit and an actively shielded triple-resonance probe. Sequential assignments of SNase were obtained from HNCACB (Wittekind & Mueller, 1993) and CBCA(CO)NNH (Grzesiek & Bax, 1992) triple-resonance experiments and from published values (Torchia *et al.*, 1989). Matrices of $64 \times 32 \times 576$ and $60 \times 32 \times 576$ complex points were acquired with spectral widths of 9178.5, 1663.0 and 9000.9 Hz (F_1, F_2 and F_3) for HNCACB and CBCA(CO)NNH, respectively. Quadrature detection in all of the indirectly detected dimensions was achieved *via* States-TPPI (Marion *et al.*, 1989). Spectra were processed using the NMRPipe software system (Delaglio *et al.*, 1995) and analyzed with NMRView software (Johnson & Blevins, 1994). Assignments of Δ131Δ and the SH3 domain (both F_S and U_{Gdn} states) have been published (Zhang *et al.*, 1994, 1997b).

^{15}N backbone relaxation

A series of inverse detected 2D ^{1}H-^{15}N NMR experiments were used to determine backbone ^{15}N T_1 and T_2 relaxation times and heteronuclear ^{1}H-^{15}N steady-state NOE values (Farrow *et al.*, 1994). Details for experiments recorded on the drkN SH3 domain are described by Farrow *et al.* (1997). In the case of SNase, T_1, T_2 and NOE spectra were recorded (600 MHz ^{1}H frequency) as 128×576 complex matrices with spectral widths of 1663.0 and 9000.9 Hz in F_1 and F_2, respectively, while for Δ131Δ, 160×576 complex matrices with spectral widths of 1400.0 and 9000.9 Hz were employed. Recycle delays for T_1 and T_2 experiments were 1.1 and 2.0 s, respectively. Values of T_1 were determined on the basis of spectra recorded with eight delays ranging from 11 to 770 ms, while T_2 values were based on seven experiments recorded with delays extending from 16.7 ms to 117 ms. To minimize contributions to T_2 from chemical exchange among different conformers, a short delay of 2×58.7 μs was employed between ^{15}N 180° pulses in CPMG-based experiments (Bloom *et al.*, 1965). In addition, in the case of Δ131Δ, a series of CPMG experiments was recorded with delays between ^{15}N 180° pulses of 2×58.7, 2×102.1, 2×188.9 and 2×449.3 μs in order to assess contributions to measured transverse relaxation times from chemical exchange. ^{1}H-^{15}N NOE values were determined from two spectra, recorded with and without ^{1}H presaturation. A recycle delay of six seconds was used for spectra recorded without ^{1}H saturation, while a three second delay followed by three seconds of ^{1}H saturation was employed in spectra recorded with the NOE. T_1 and T_2 values were calculated from a non-linear least-squares fit of measured cross-peak intensities to a function of the form:

$$I(t) = I(0)\exp(-t/T_i) \tag{20}$$

where T_i ($i = 1$ and 2) is the relevant relaxation time and $I(t)$ is the intensity of a given cross-peak at time t. NOE values were determined from the ratio of peak heights obtained in spectra recorded with and without proton saturation. Errors in T_i and NOE values were obtained as described (Farrow *et al.*, 1997).

Data analysis

^{15}N T_1, T_2 and ^{1}H-^{15}N steady-state NOE data were analyzed in the manner described in the main text. Values of (S'^2, τ'_M, τ'_e) for each residue were obtained from a separate fitting of relaxation parameters for each residue. Residues fit with $\tau'_e \geqslant 0.3$ ns were not included in further analysis. S'^2 values obtained by the method described were compared in the case of the F_S state of the drkN SH3 domain with S^2 values generated by using the global optimum τ_M values of 4.5 ns (30°C) and 6.3 ns (14°C), obtained previously (Farrow *et al.*, 1997), and an S^2-τ_e spectral density model to describe the relaxation data. The pairwise root-mean-squared deviation (r.m.s.d) of S^2 values obtained from the two approaches for data recorded at 14 and 30°C is 0.006 and 0.014, respectively. In the case of ^{15}N relaxation data from ubiquitin analyzed assuming diffusion anisotropy the pairwise r.m.s.d of the S^2 values reported by Tjandra *et al.* (1995) and S'^2 values is 0.008. Standard deviations in the parameters (S'^2, τ'_M, τ'_e) were obtained by noting that for a function, $f(T_1,T_2,\text{NOE})$, the error in f is given by:

$$\begin{aligned} df = \{&[(\partial f/\partial T_1)(dT_1)]^2 + [(\partial f/\partial T_2)(dT_2)]^2 \\ &+ [(\partial f/\partial \text{NOE})(d\text{NOE})]^2\}^{0.5} \end{aligned} \tag{21}$$

where dT_1, dT_2 and dNOE are the errors in T_1, T_2 and NOE values, respectively, and f is one of (S'^2, τ'_M, τ'_e). If dT_1 is much smaller than T_1, $[(\partial f/\partial T_1)(dT_1)]^2$ can be approximated by:

$$\begin{aligned} [(\partial f/\partial T_1)(dT_1)]^2 \approx &[\{f(T_1 + dT_1, T_2, \text{NOE}) - f(T_1, T_2, \text{NOE})\}^2 \\ &+ \{f(T_1 - dT_1, T_2, \text{NOE}) \\ &- f(T_1, T_2, \text{NOE})\}^2]/2 \end{aligned} \tag{22}$$

with similar equations holding for T_2 and NOE.

^{2}H relaxation times

Pulse schemes and experimental setup for the measurement of ^{2}H T_1 and $T_{1\rho}$ relaxation times are given by Muhandiram *et al.* (1995) and Kay *et al.* (1996). All spectra were recorded at a field strength of 600 MHz. Each correlation spectrum consisted of a data matrix of 96×1152 complex points with acquisition times of 22.8 and 64 ms in t_1 and t_2, respectively. In order to obtain $T_1(I_ZC_ZD_Z)$ values, eight 2D ^{13}C-^{1}H correlation spectra with delays of 0.05, 4.3, 9.0, 14.4, 20.4, 27.4, 35.7 and 45.0 ms were acquired (30°C). Values of $T_{1\rho}(I_ZC_ZD_Y)$ were based on eight spectra recorded with delays of 0.2, 1.4, 3.0, 4.8, 6.8, 9.2, 11.9 and 15.0 ms. Values of $T_1(I_ZC_Z)$ were measured using spectra recorded with the same delays as for $T_1(I_ZC_ZD_Z)$. Relaxation times of pure deuterium magnetization, D_Z and D_Y, can be readily extracted from the relations:

$$\begin{aligned} 1/T_1(D_Z) &= 1/T_1(I_ZC_ZD_Z) - 1/T_1(I_ZC_Z) \\ 1/T_{1\rho}(D_Y) &= 1/T_{1\rho}(I_ZC_ZD_Y) - 1/T_1(I_ZC_Z) \end{aligned} \tag{23}$$

as described in detail by Muhandiram *et al.* (1995) and Yang & Kay (1996b) and ^{2}H relaxation times related to motional parameters *via*:

$$1/T_1 = (3/40)(e^2qQ/\hbar)^2[J(\omega_D) + 4J(2\omega_D)] \tag{24}$$

$$1/T_{1\rho} = (1/80)(e^2qQ/\hbar)^2[9J(0) + 15J(\omega_D) + 6J(2\omega_D)]$$

with $J(\omega)$ defined by:

$$J(\omega) = S^2\tau_M/(1+\omega^2\tau_M^2) + (1-S^2)\tau_e/(1+\omega^2\tau_e^2) \qquad (25)$$

where τ_M is the overall tumbling time of the molecule, S is an order parameter for the methyl group describing the spatial restriction of motion of the ^{13}C-^2H bond vector, τ_e describes the internal motions of the bond vector and e^2qQ/h is the quadrupole coupling constant (168 kHz for methyl deuterons (Burnett & Muller, 1971)). Assuming tetrahedral geometry for the methyl group, S^2 can be related to S^2_{axis} by the relation $S^2 = 0.111\ S^2_{axis}$ (Nicholson *et al.*, 1992). τ_M values of 9.00(±0.06) ns (5°C), 6.62(±0.03) ns (14°C) and 4.21(±0.02) ns (30°C) have been used in the data analysis, obtained from backbone ^{15}N relaxation data recorded on the sample used for ^2H relaxation measurements.

Acknowledgements

This research was supported by the National Cancer Institute of Canada (L.E.K. and J.D.F.), the National Sciences and Engineering Research Council of Canada (L.E.K.), the Protein Engineering Center of Excellence (L.E.K.) and the Medical Research Council of Canada (J.D.F.). N.A.F. is a research fellow of the National Cancer Institute of Canada supported with funds provided by the Terry Fox Run. L.E.K. thanks Professor David Shortle, Johns Hopkins, for the very generous supply of SNase and Δ131Δ protein samples, and Professors Shortle, Josh Wand, SUNY Buffalo, and Ernesto Freire, Johns Hopkins, for stimulating discussions and encouragement. L.E.K. is an Alfred P. Sloan Research Fellow and an International Research Scholar of the Howard Hughes Medical Research Institute.

References

Abragam, A. (1961). *Principles of Nuclear Magnetism.* Clarendon Press, Oxford.

Akke, M., Bruschweiler, R. & Palmer, A. (1993). NMR order parameters and free energy: an analytic approach and application to cooperative calcium binding by calbindin D9k. *J. Am. Chem. Soc.* **115**, 9832–9833.

Alexandrescu, A. T. & Shortle, D. (1994). Backbone dynamics of a highly disordered 131 residue fragment of staphylococcal nuclease. *J. Mol. Biol.* **242**, 527–546.

Alexandrescu, A. T., Abeygunawardana, C. & Shortle, D. (1994). Structure and dynamics of a denatured 131-residue fragment of staphylococcal nuclease: a heteronuclear NMR study. *Biochemistry,* **33**, 1063–1072.

Bax, A. (1994). Multidimensional nuclear magnetic resonance methods for protein studies. *Curr. Opin. Struct. Biol.* **4**, 738–744.

Bloom, M., Reeves, L. W. & Wells, E. J. (1965). Spin echoes and chemical exchange. *J. Chem. Phys.* **42**, 1615–1624.

Broadhurst, R. W., Hardman, C. H., Thomas, J. O. & Laue, E. D. (1995). Backbone dynamics of the A-domain of HMG1 as studied by ^{15}N NMR spectroscopy. *Biochemistry,* **34**, 16608–16617.

Bruschweiler, R., Liao, X. & Wright, P. E. (1995). Long-range motional restrictions in a multidomain zinc-finger protein from anisotropic tumbling. *Science,* **268**, 886–889.

Burnett, L. H. & Muller, B. H. (1971). Deuteron quadrupole coupling constants in three solid deuterated paraffin hydrocarbons: C_2D_6, C_4D_{10}, C_6D_{14}. *J. Chem. Phys.* **55**, 5829–5831.

Delaglio, F., Grzesiek, S., Vuister, G. W., Zhu, G., Pfeifer, J. & Bax, A. (1995). NMRPipe: a multidimensional spectral processing system based on UNIX pipes. *J. Biomol. NMR,* **6**, 277–293.

Eisenberg, D. & Crothers, D. (1979). *Physical Chemistry with Applications to the Life Sciences.* The Benjamin/Cummings Publishing Co, Inc., Menlo Park, CA.

Farrow, N. A., Muhandiram, R., Singer, A. U., Pascal, S. M., Kay, C. M., Gish, G., Shoelson, S. E., Pawson, T., Forman-Kay, J. D. & Kay, L. E. (1994). Backbone dynamics of a free and phosphopeptide-complexed src homology 2 domain studied by ^{15}N NMR relaxation. *Biochemistry,* **33**, 5984–6003.

Farrow, N. A., Zhang, O., Forman-Kay, J. D. & Kay, L. E. (1995a). Comparison of the backbone dynamics of a folded and an unfolded SH3 domain existing in equilibrium in aqueous buffer. *Biochemistry,* **34**, 868–878.

Farrow, N. A., Zhang, O., Szabo, A., Torchia, D. A. & Kay, L. E. (1995b). Spectral density function mapping using ^{15}N relaxation data exclusively. *J. Biomol. NMR,* **6**, 153–162.

Farrow, N. A., Zhang, O., Forman-Kay, J. D. & Kay, L. E. (1997). Characterization of the backbone dynamics of folded and denatured states of an SH3 domain. *Biochemistry,* **36**, 2390–2402.

Flanagan, J. M., Kataoka, M., Shortle, D. & Engelman, D. M. (1992). Truncated staphylococcal nuclease is compact but disordered. *Proc. Natl Acad. Sci. USA,* **89**, 748–752.

Gillespie, J. & Shortle, D. (1997). Characterization of long range structure in the denatured state of staphylococcal nuclease. II. Distance restraints from paramagnetic relaxation and calculation of an ensemble of structures. *J. Mol. Biol.* **268**, 170–184.

Gomez, J., Hilser, V. J., Xie, D. & Freire, E. (1995). The heat capacity of proteins. *Proteins: Struct. Funct. Genet.* **22**, 404–412.

Grzesiek, S. & Bax, A. (1992). Correlating backbone amide and side chain resonances in larger proteins by multiple relayed triple resonance NMR. *J. Am. Chem. Soc.* **114**, 6291–6293.

Ishima, R. & Nagayama, K. (1995). Quasi-spectral-density function analysis for nitrogen-15 nuclei in proteins. *J. Magn. Reson. ser. B,* **108**, 73–76.

Johnson, B. A. & Blevins, R. A. (1994). NMRView: a computer program for the visualization and analysis of NMR data. *J. Biomol. NMR,* **4**, 603–614.

Kay, L. E., Torchia, D. A. & Bax, A. (1989). Backbone dynamics of proteins as studied by ^{15}N inverse detected heteronuclear NMR spectroscopy: application to staphylococcal nuclease. *Biochemistry,* **28**, 8972–8979.

Kay, L. E., Muhandiram, D. R., Farrow, N. A., Aubin, Y. & Forman-Kay, J. D. (1996). Correlation between dynamics and high affinity binding in an SH2 domain interaction. *Biochemistry,* **35**, 361–368.

LeMaster, D. M. & Kushlan, D. M. (1996). Dynamical mapping of *E. coli* thioredoxin via ^{13}C NMR relaxation analysis. *J. Am. Chem. Soc.* **118**, 9255–9264.

Li, Z., Raychaudhuri, S. & Wand, A. J. (1996). Insights into the local residual entropy of proteins provided by NMR relaxation. *Protein Sci.* **5**, 2647–2650.

Lipari, G. & Szabo, A. (1982a). Model-free approach to the interpretation of nuclear magnetic relaxation in macromolecules. 1. Theory and range of validity. *J. Am. Chem. Soc.* **104**, 4546–4559.

Lipari, G. & Szabo, A. (1982b). Model-free approach to the interpretation of nuclear magnetic relaxation in macromolecules. 2. Analysis of experimental results. *J. Am. Chem. Soc.* **104**, 4559–4570.

Logan, T. M., Theriault, Y. & Fesik, S. W. (1994). Structural characterization of FK506 binding protein unfolded in urea and GdnHCl. *J. Mol. Biol.* **236**, 637–648.

Loll, P. J. & Lattman, E. E. (1989). The crystal structure of the ternary complex of staphylococcal nuclease, Ca^{2+}, and the inhibitor pdTp, refined at 1.65 Å. *Proteins: Struct. Funct. Genet.* **5**, 183–201.

Makhatadze, G. I. & Privalov, P. L. (1990). Heat capacity of proteins. I. Partial molar heat capacity of individual amino acid residues in aqueous solution: hydration effect. *J. Mol. Biol.* **213**, 375–384.

Mandel, A. M., Akke, M. & Palmer, A. G. (1996). Dynamics of ribonuclease H: temperature dependence of motions on multiple time scales. *Biochemistry,* **35**, 16009–16023.

Marion, D., Ikura, M., Tschudin, R. & Bax, A. (1989). Rapid recording of 2D NMR spectra without phase cycling. Application to the study of hydrogen exchange in proteins. *J. Magn. Reson.* **85**, 393–399.

Muhandiram, D. R., Yamazaki, T., Sykes, B. D. & Kay, L. E. (1995). Measurements of deuterium T_1 and T_1r relaxation times in uniformly ^{13}C labeled and fractionally deuterium labeled proteins in solution. *J. Am. Chem. Soc.* **117**, 11536–11544.

Nicholson, L. K., Kay, L. E., Baldisseri, D. M., Arango, J., Young, P. E., Bax, A. & Torchia, D. A. (1992). Dynamics of methyl groups in proteins as studied by proton-detected ^{13}C NMR spectroscopy. Application to the leucine residues of staphylococal nuclease. *Biochemistry,* **31**, 5253–5263.

Novokhatny, V. & Ingham, K. C. (1994). Domain structure of the fib-1 and fib-2 fragments of fibronectin: thermodynamic properties of the finger module. *J. Mol. Biol.* **238**, 833–844.

Palmer, A. G., Rance, M. & Wright, P. E. (1991). Intramolecular motions of a zinc finger DNA-binding domain from Xfin characterized by proton-detected natural abundance ^{13}C heteronuclear NMR spectroscopy. *J. Am. Chem. Soc.* **113**, 4371–4380.

Peng, J. W. & Wagner, G. (1992). Mapping of the spectral densities of N-H bond motions in Eglin c using heteronuclear relaxation experiments. *Biochemistry,* **31**, 8571–8586.

Philippopoulos, M. & Lim, C. (1995). Molecular dynamics simulation of *E. coli* ribonuclease H1 in solution: correlation with NMR and X-ray data and insights into biological function. *J. Mol. Biol.* **254**, 771–792.

Privalov, P. L. & Gill, S. J. (1988). Stability of protein structure and hydrophobic interaction. *Advan. Protein Chem.* **39**, 191–234.

Privalov, P. L. & Makhatadze, G. I. (1990). Heat capacity of proteins. II. Partial molar heat capacity of the unfolded polypeptide chain of proteins: protein unfolding effects. *J. Mol. Biol.* **213**, 385–391.

Schneider, D. M., Dellwo, M. J. & Wand, A. J. (1992). Fast internal main-chain dynamics of human ubiquitin. *Biochemistry,* **31**, 3645–3652.

Schurr, J. M., Babcock, H. P. & Fujimoto, B. S. (1994). A test of the model-free formulas. Effects of anisotropic rotational diffusion and dimerization. *J. Magn. Reson. ser. B,* **105**, 211–224.

Shortle, D. (1996). Structural analysis of non-native states of proteins by NMR methods. *Curr. Opin. Struct. Biol.* **6**, 24–30.

Sosnick, T. R. & Trewhella, J. (1992). Denatured states of ribonuclease A have compact dimensions and residual secondary structure. *Biochemistry,* **31**, 8329–8335.

Tjandra, N., Feller, S. E., Pastor, R. W. & Bax, A. (1995). Rotational diffusion anisotropy of human ubiquitin from ^{15}N NMR relaxation. *J. Am. Chem. Soc.* **117**, 12562–12566.

Torchia, D. A., Sparks, S. W. & Bax, A. (1989). Staphylococcal nuclease: sequential assignments and solution structure. *Biochemistry,* **28**, 5509–5524.

van Mierlo, C. P. M., Darby, N. J., Keeler, J., Neuhaus, D. & Creighton, T. E. (1993). Partially folded conformation of the (30-51) intermediate in the disulphide folding pathway of bovine pancreatic trypsin inhibitor. *J. Mol. Biol.* **229**, 1125–1146.

Wittekind, M. & Mueller, L. (1993). HNCACB, a high sensitivity 3D NMR experiment to correlate amide proton and nitrogen resonances with the alpha- and beta-carbon resonances in proteins. *J. Magn. Reson. ser. B,* **101**, 201–205.

Woessner, D. E. (1962). Nuclear spin relaxation in ellipsoids undergoing rotational brownian motion. *J. Chem. Phys.* **37**, 647–654.

Wüthrich, K. (1986). *NMR of Proteins and Nucleic Acids.* John Wiley & Sons, New York.

Yang, D. & Kay, L. E. (1996a). Contributions to conformational entropy arising from bond vector fluctuations measured from NMR-derived order parameters: application to protein folding. *J. Mol. Biol.* **263**, 369–382.

Yang, D. & Kay, L. E. (1996b). The effects of cross correlation and cross relaxation on the measurement of deuterium T_1 and $T_{1\rho}$ relaxation times in $^{13}CH_2D$ spin systems. *J. Magn. Reson. ser. B,* **110**, 213–218.

Zhang, O. & Forman-Kay, J. D. (1995). Structural characterization of folded and unfolded states of an SH3 domain in equilibrium in aqueous buffer. *Biochemistry,* **34**, 6784–6794.

Zhang, O., Kay, L. E., Olivier, J. P. & Forman-Kay, J. D. (1994). Backbone ^1H and ^{15}N resonance assignments of the N-terminal SH3 domain of drk in folded and unfolded states using enhanced-sensitivity pulsed field gradients NMR techniques. *J. Biomol. NMR,* **4**, 845–858.

Zhang, O., Forman-Kay, J. D., Shortle, D. & Kay, L. E. (1997a). Triple-resonance NOESY-based experiments with improved spectral resolution: applications to structural characterization of unfolded, partially folded and folded proteins. *J. Biomol. NMR,* **9**, 181–200.

Zhang, O., Kay, L. E., Shortle, D. & Forman-Kay, J. D. (1997b). Comprehensive NOE characterization of a

partially folded large fragment of staphylococcal nuclease, Δ131Δ, using NMR methods with improved resolution. *J. Mol. Biol.* In the press.

Zheng, Z., Czaplicki, J. & Jardetzky, O. (1995). Backbone dynamics of trp repressor studied by ^{15}N NMR relaxation. *Biochemistry,* **15**, 5212–5223.

Edited by P. E. Wright

(Received 12 May 1997; received in revised form 11 July 1997; accepted 14 July 1997)